

Multi-Lane Coordinated Control Strategy of Connected and Automated Vehicles for On-Ramp Merging Area Based on Cooperative Game

Lan Yang^{ID}, Jiahao Zhan, Wen-Long Shang^{ID}, Member, IEEE, Shan Fang, Guoyuan Wu^{ID}, Senior Member, IEEE, Xiangmo Zhao^{ID}, Member, IEEE, and Muhammet Deveci^{ID}

Abstract—Ramp merging represents a bottleneck scenario that causes traffic congestion, accidents, and increases emissions. Connected and Automated Vehicles (CAVs) can realize the coordinated control of ramp merging through vehicle-to-infrastructure (V2I) for relieving above problems. Considering the previous studies on centralized ramp merging only involved single mainline, this paper proposes a multi-lane centralized collaborative control strategy using cooperative game. First, the merging rules of different lanes of vehicles in the merging area are defined, so that the vehicles can achieve the cooperative merging safely. Second, driving efficiency, comfort, and fuel consumption in the merging control zone are used as the cost function. The best merging sequences of vehicles in different lanes are solved by cooperative game. Finally, analytical solution of longitudinal optimal control for all vehicles is obtained by applying the Pontryagin principle. The effectiveness of the proposed method is verified through simulation under random traffic conditions. Compared to other centralized control algorithms, it can significantly improve driving efficiency and reduce fuel consumption. At the same time, the applicability of the method is verified by comparing with ExiD datasets, and some advantages are obtained in terms of fuel consumption.

Index Terms—CAVs, cooperative game, optimal control, multi-lane merging, on-ramp.

Manuscript received 29 October 2022; revised 25 March 2023; accepted 25 April 2023. Date of publication 5 June 2023; date of current version 1 November 2023. This work was supported in part by the National Key Research and Development Program of China under Grant 2021YFB2501200, in part by the National Natural Science Foundation of China under Grant 61703053, in part by the Beijing Natural Science Foundation under Grant L211027 and Grant 9232003, and in part by the Shaanxi Province Key Research and Development Program under Grant 2022GY-300. The Associate Editor for this article was H. Lv. (*Corresponding author: Wen-Long Shang*)

Lan Yang, Jiahao Zhan, Shan Fang, and Xiangmo Zhao are with the School of Information Engineering, Chang'an University, Xi'an 710064, China (e-mail: lanyang@chd.edu.cn; Z1730152624@163.com; fang6100146@163.com; xmzhao@chd.edu.cn).

Wen-Long Shang is with the School of Traffic and Transportation, Beijing Jiaotong University, Beijing 100091, China, also with the Beijing Key Laboratory of Traffic Engineering, College of Metropolitan Transportation, Beijing University of Technology, Beijing 100124, China, and also with the Centre for Transport Studies, Imperial College London, SW7 2BX London, U.K. (e-mail: shangwl_imperial@bjut.edu.cn).

Guoyuan Wu is with the Center for Environmental Research and Technology, University of California at Riverside, Riverside, CA 92521 USA (e-mail: gywu@cert.ucr.edu).

Muhammet Deveci is with the Royal School of Mines, Imperial College London, SW7 2AZ, London, U.K., and also with the Department of Industrial Engineering, Turkish Naval Academy, National Defence University, 34940 Istanbul, Turkey (e-mail: muhammetdeveci@gmail.com).

Digital Object Identifier 10.1109/TITS.2023.3275055

I. INTRODUCTION

A. Motivation

THE on-ramp merging area is a typical bottleneck in the highway network, because the merging of the on-ramp vehicles may seriously interfere with the main line traffic flow and have various negative effects on traffic efficiency and safety [1]. Due to the mandatory lane change of on-ramp vehicles, the decision-making interaction between the vehicles may lead to frequent stop-go phenomena, which create a series of safety and fuel consumption problems. At the same time, when there is only single mainline, the traffic efficiency in the merging area is further reduced.

The continuous development of vehicle infrastructure cooperative has provided a new development direction for decision making and control of CAVs. With the increase of CAV penetration, information exchange by means of Internet of vehicle [2], [3] has become an important way to solve conflicts and fuel consumption problems in different traffic scenarios [4], [5], [6], [7].

CAV centralized control based on V2I is also widely used in on-ramp merging research. However, the research on ramp merging for CAVs decision-making control mainly focuses on collaboration scenarios with single mainline [8], [9], [10], [11], [12], [13], [14], [15], [16], [17], [18], [19]. It seriously ignores the decision-making factors that vehicles on the outside of the mainline may change lanes under the real multi-lane merging scenario, which dramatically reduces road utilization and results in more fuel consumption [20], [21]. Therefore, it is significant to consider the real collaborative decision-making of CAVs from the perspective of actual merging scenarios.

B. Literature Review

To achieve the coordinated control of vehicles in the ramp merging area, it is necessary to determine the appropriate merging sequence (MS) and generate a reasonable vehicle trajectory [22]. The existing literatures on coordinated merging has two kinds of types: rule-based and optimization-based [10].

In the rule-based approach, the MS of vehicles are first determined according to specific rules; then, the trajectory for each vehicle is planned. Existing coordination rules for vehicles are usually defined by heuristic rules such as first-in

first-out (FIFO) [11], [12], [13] or fuzzy logic rules [14], [15]. Generally, these rules are based on vehicle behavior and lane characteristics in the merging area. Considering the acceleration and deceleration behavior of vehicles, Zhou et al. [16] proposed an on-ramp controller based on the collaborative intelligent driver model to solve the problem of traffic oscillation and efficiency in merging zone. Xue et al. [17] proposed a platoon-based rule to form a platoon of ramp vehicles with the same pre target merging gap to determine MS and improve merging efficiency. Similar platoon rules can also be applied on the mainline to determine the lane selection of ramp vehicles [18]. The rule algorithm will also be adjusted to meet the requirements of the merge. In research [19], the optimal MS of the ramp vehicle is adjusted by balancing computational cost, and fuel consumption. However, the MS of the vehicle under these rules was temporary and could not ensure global optimization.

In the optimization-based method, the MS of the vehicle is determined by minimizing the objective function through some optimization algorithms. Such merging methods usually include optimal control algorithm [23], [24] and MPC algorithm [25], [26]. The optimal control strategy aims at reducing fuel consumption and improving comfort, thus further coordinating the optimal MS for vehicles in the merging area [27], [28]. MPC further realizes the adjustment of vehicle merging trajectory according to the vehicle motion characteristics [29]. In addition, in order to solve the MS problem of ramp merging areas from the traffic level, many studies have optimized the throughput and delay of traffic from the perspective of macro merging models [30]. In research [31], the combined travel delay of on-ramp vehicles under different traffic flows was optimized by taking the travel time of ramp and mainline vehicles as a cost function. Liu further analyzed the unevenness of traffic flow between lanes and established a lane selection model to achieve the merging and selection of ramp vehicles [32]. However, the above optimization methods are often one-sided when considering the driving factors of vehicles. Furthermore, the targets of optimization are not comprehensive, and the optimized objects of certain methods are also relatively singular, in that they do not analyze and discuss the merging of multiple vehicles in the merging area.

Strategy research based on game theory is widely adopted in traffic decision making [33]. Game theory can determine the best decision result from a series of strategic choices by analyzing the costs and benefits for each participant to compete or cooperate. Therefore, game theory can also be viewed as a combination of rule-based and optimization methods [34], [35]. From the perspective of competition, non-cooperative game is most widely used [36], [37]. Among them, Kita [38] is the first to use non-zero sum non-cooperative game to solve the vehicle merging problem. He reflected the game benefits of vehicles through different time variables. Wei et al. [39] proposed a ramp merging behavior control system based on game theory, and used Stackelberg game to simulate the decision-making interaction of vehicles on two lanes. However, these non-cooperative game models focus only upon the driving benefits of individual vehicles, while cooperative games often achieve win-win or even multi-win situations

among participants and yield positive social benefits. As cooperative game requires collaborative communication between CAVs, literature [40] determines the decision-making interaction of merging vehicles through different game modes in the mixed traffic flow merging environment. In the full CAVs environment, the interactive vehicles in the merging area can achieve the optimal MS by minimizing the cost or maximizing the payoff under the cooperative game [41], [42].

Reviewing the above literatures, both the rule-based and optimization-based methods can effectively obtain the MS of vehicles in the merging area. However, most of the scenarios only involve the interaction behavior of vehicles on the ramp and the single lane of the mainline, without considering the possibility of vehicles changing lanes in the real merging decision-making process when the mainline has multiple lanes, which is inconsistent with the actual driving situation and reduces the utilization rate of lanes; Or they describe the traffic efficiency of vehicles passing through the ramp merging area under high flow from a macro perspective, without considering the multi-objective demand of individual vehicles when merging. At the same time, in view of the fact that cooperative games can achieve win-win results among game participants, the above merging games are not comprehensive in terms of the driver's benefit or cost, and cannot better reflect the decision-making demands. Therefore, it is necessary to determine the MS of CAVs in multi-lane from the perspective of games and optimizations in a real scenario.

C. Contribution of the Paper

In this paper, we combine cooperative game with optimal control method to propose a decision-making method for the merging of vehicles on multi-lane. The main contributions of this paper are: (1) A two-lane mainline and single-lane ramp scenario is proposed by real road scene, and two merging points are established on mainline to solve the MS and optimization problems in the control zone; (2) An objective optimization function including vehicle efficiency, fuel consumption and driving comfort is proposed. The MS is solved by cooperative game, and the analytical solution of vehicle motion is derived by optimal control; (3) The applicability of the model is verified through multi-lane merging simulation experiments, and the validity of the model is verified by comparison against merging scenarios obtained from a real dataset.

D. Organization of the Paper

This paper is organized as follows: Section II formulates a multi-lane merging scenario and provides the corresponding methodology for the merging strategy, Section III illustrates the solutions of the cooperative game and optimal control, Section IV introduces the simulation and comparison results, and the conclusion and future work are given in Section V.

II. PROBLEM FORMULATION AND METHODOLOGY

A. System Description

As shown in Fig. 1, a two-mainline and single-ramp merging scenario is defined. Suppose that there is a central controller in

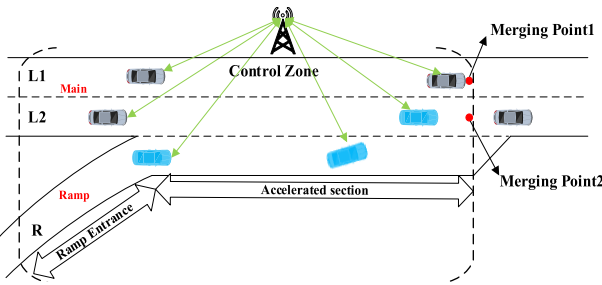


Fig. 1. On-ramp merge scenario for multi-lane road.

this merging section, and all CAVs passing through the control zone are controlled by it. And two merging points (MP) in Lane L1 and L2. The MP2 is used to realize the merging of vehicles on L2 and ramp. In order to ensure consistent longitudinal control length, MP1 is the vertical mapping point of MP2, which is used for merging of vehicles on L2 and L1. And MP1 can only be considered when L2 vehicles change lanes.

Once CAVS vehicles have entered the control area, their state information is captured by the central controller, which oversees the road characteristics in the control area. The vehicle motion constraints in this area are as follows:

1) Vehicles in the control area are not allowed to make continuous lane changes and overtake. To avoid increasing the pressure in L2, vehicles on L1 are not allowed to change lanes to L2. It is worth noting that when the number of vehicles distributed in the three lanes is large and the time of vehicles entering the control area is similar, the central controller will carry out this guidance constraint on vehicles on L1.

2) When the ramp vehicles merging with the vehicles on L2, if L1 satisfies the lane-changing conditions of the vehicles on L2, the vehicles on L2 can change lanes to L1.

Therefore, L1 can offer lane-changing strategies for vehicles on L2, to facilitate the safer merging of ramp vehicles on the mainline and further improve the lane utilization rate.

For each vehicle entering the control area, the central controller numbers them according to the entering time sequence. The state equation for vehicle i in the control area is:

$$\dot{\mathbf{x}}_i(t) = f(\mathbf{x}_i(t), \mathbf{u}_i(t), t) \quad (1)$$

where t denotes the time, $\dot{\mathbf{x}}_i(t)$ represents the vehicle state vector, and $\mathbf{u}_i(t)$ represents the vehicle control vector. The state vector $\dot{\mathbf{x}}_i(t)$ is represented by the third-order kinematics equation $\dot{\mathbf{x}}_i(t) = [x_i(t), v_i(t), a_i(t)]^T$, which expresses the position, velocity, and acceleration of vehicle i , respectively. This set of above is a bounded subset of the real number R , and $\mathbf{u}_i(t)$ is the jerk of the vehicle, which satisfies

$$[\dot{x}_i(t), \dot{v}_i(t), \dot{a}_i(t)] = [v_i(t), a_i(t), u_i(t)] \quad (2)$$

Meanwhile, to ensure that the vehicles' motion state and control input are within a reasonable range, the following constraints are defined for the vehicle's velocity, acceleration, and jerk: $v_i(t) \in [0, v_{max}]$, $a_i(t) \in [a_{min}, a_{max}]$, $u_i(t) \in [u_{min}, u_{max}]$.

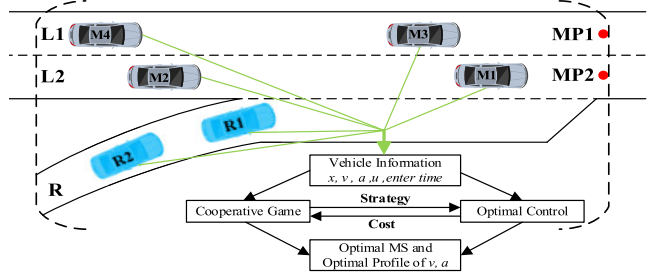


Fig. 2. Merging under information exchange.

B. Multi-Lane Merging Decision Based on Cooperative Game

A cooperative game consists of the following six elements: player N , strategy S , action A , payoff or cost U , information I , and equilibrium E . During the merging process, the central controller coordinates all vehicles in the control area; hence, the information I for all vehicles is known. The vehicles that interact in control zone are game players N , and strategy S_i represents the strategy set that vehicle i can choose before arriving the merging point. When players make specific action A , the corresponding benefit or cost U_i is calculated through the subsequent cost function. Due to the goal of each player is to choose the strategy that minimizes the cost or maximizes the payoff in the merging area; that is, the equilibrium solution E must satisfy the cost minimization or payoff maximization.

In the merging scenario, the central controller must arrange the MS of the CAVs entering the control area. Due to the different costs incurred by different strategies, the action of CAVs will vary according to the actual situation. Therefore, in order to solve the conflict problem in the control area and promote the multi-win situation of vehicles, we use cooperative game to model the merging decision-making of CAVs in the control area, and minimize the global cost through optimal control to achieve the optimal MS.

Figure 2 shows the information exchange process between the vehicle and the central controller in the control area. The central controller will record the initial time when vehicles enter the control zone, and the vehicles will also share their own motion information to the central controller, and obtain the optimal MS, speed profile and acceleration profile through cooperative game and optimal control method.

Since the main task of the central controller is to solve the merging problem of ramp vehicles, when the vehicles on L2 do not choose the lane change strategy, the vehicles passing through MP1 are only vehicles on L1, and the MS of MP1 is FIFO sequence. For ramp vehicle and vehicle on L2, their game strategy is expressed as follows: when ramp vehicle R arrives at MP2, its strategy $S_R = \{\text{be the leader; be the follower}\}$. And the strategies of vehicle M on L2 are $S_M = \{\text{be the leader; be the follower; change lane to L1}\}$. Therefore, the cooperative game matrix for vehicles in the two lanes is as presented in Table I.

Due to vehicles can only pass MP in the same lane in sequence or from different lanes, the cost of deciding between "be the leader" or "be the follower" simultaneously for the

TABLE I
GAME COST MATRIX OF VEHICLES PASSING MP2

Roles	Ramp Vehicles(R)		
	Strategies	Leader(L)	Follower(F)
L2	Leader(L)	(U _{ML} , U _{RL})	(U _{ML} , U _{RF})
	Follower(F)	(U _{MF} , U _{RL})	(U _{MF} , U _{RF})
	Lane-Changing (LC)	(U _{MLC} , U _{RL})	(U _{MLC} , U _{RF})

two vehicles in Table I is ∞ , because it will inevitably cause collisions. For the vehicles on L2, if the ramp vehicles choose “be the follower” and the vehicles on L2 still choose “change lane,” the cost of the strategy combination will exceed that of {ramp vehicles be the leader; L2 vehicles change lane}. Therefore, only three of the six strategy combinations mentioned above need to be analyzed.

If the vehicle on L2 chooses the lane-changing strategy after playing with the on-ramp vehicle, then it needs to continue to play with the vehicle on L1 to achieve the optimal MS of MP1. At this time, the strategy choice for vehicles on L1 and L2 is who should be the leader or follower.

C. Cost Function in the Cooperative Game

Before considering the cost function of the game, in order to form a stable platoon through the merging point, we make some assumptions regarding the motion states of vehicles, based upon safety considerations:

Assumption 1: After passing the merging point, each vehicle travels at a constant velocity for a period of time; that is, the acceleration of a vehicle at the merging point is zero.

Assumption 2: The headway of vehicles in the same lane passing through the merging point is constant; that is, $t_f^{i-1} = t_f^i + T_s$, where t_f^i and t_f^{i-1} represent the time at which vehicles i and $i-1$ pass through the merging point, and T_s is a fixed headway.

When the central controller coordinates the vehicle platoon, a vehicle must first pass through the corresponding merging point (as shown by the M1 and M3 vehicles in Fig. 2). Assuming that the heading vehicle always travels in front of the merging point, the arriving time of the heading vehicle can be confirmed by the central controller. Once the arriving time of the heading vehicles at the two merging points is determined, the arriving time of other vehicles can also be determined.

Therefore, in the merging process considered by the central controller, the cost in the control area is minimized primarily by coordinating the time sequence of the vehicles passing through the merging point. Simultaneously, considering the needs of different vehicles, we establish (i) a longitudinal cost function that comprehensively considers vehicle efficiency, fuel consumption, and comfort and (ii) a lateral cost function that considers vehicle lane-changing comfort; these are shown in

$$J_{lon} = \frac{1}{2} \int_{t_0}^{t_f} (\omega_1 (v_x - v_{des})^2 + \omega_2 a_x^2 + \omega_3 u_x^2) dt \quad (3)$$

$$J_{lat} = \frac{1}{2} \int_{t_1}^{t_{LC}} u_y^2 dt \quad (4)$$

respectively. In Eq. (3), t_0 is the time when the vehicle enters the control area, t_f is the time when the vehicle arrives at MP1 or MP2. v_{des} is the expected velocity. When the road has a maximum velocity limit, the central controller can set expected velocity as this value. v_x , a_x , and u_x are the longitudinal velocity, acceleration and jerk, respectively. The three terms in the longitudinal cost function reflect the efficiency, fuel and comfort costs of the vehicles, respectively. Reducing the difference between the current and expected velocities can improve the efficiency of the vehicle, reducing the acceleration $a(t)$ can indirectly reduce the fuel consumption, and reducing jerk $u(t)$ can improve the driving comfort. ω_1 , ω_2 , and ω_3 are the weight values of the three costs, respectively.

In the lateral cost expression Eq. (4), ramp vehicles perform mandatory lane changing; hence, their lateral costs are not considered. The possible behavior of the vehicles on L2 is discretionary lane-changing, that is, they determine whether to change lanes (and thereby incur lateral costs) according to different selection strategies. And t_1 and t_{LC} are the starting and ending times of the vehicle lane change. It is worth noting that since the game takes the time interval as the decision variable, the value of the game cost determines the time when the vehicles arrive at the merging point, so that the MS is different. Therefore, the vehicles on L2 must have the ability to change lanes. As for the values of t_1 and t_{LC} , we do not discuss them in detail in this paper, but take their difference as the lane changing time. And the difference value is generally 4-6s. For specific t_1 and t_{LC} , we will discuss them through specific lateral planning in the future.

Meanwhile, in order to save the computing resources, the game demand problem is further explained. Generally speaking, the distance between two vehicles on a highway is not recommended to be less than 100m. However, in the actual congested road conditions, it is difficult to achieve. First, the adjacent vehicles entering the control area from adjacent lanes are defined as $i-1$ and i (the time they enter the control area are t_0^{i-1} and t_0^i), and the distance and speed thresholds are 100m and v_{des} , respectively. Set the maximum initial time interval $T_{hd0} = \max(t_0^{i-1} - t_0^i) = \frac{100}{v_{des}}$. When the time interval between preceding and following vehicles of adjacent lanes entering the control zone is larger than T_{hd0} , the two vehicles will not have game demand. Conversely, new vehicles entering the control area will continue to participate in the current game.

III. SOLUTION

A. Game Solution Based on Multi-Vehicle

The multiplayer game is decomposed into multiple two-player cooperative game form. According to the game order, the ramp vehicle first play with the vehicle on L2 to obtain the cost of the two vehicles about {be the leader} and {be the follower}. Simultaneously, we consider the possibility that vehicles on L2 change lanes to L1, and we conduct game analysis on L2 and L1 vehicles. Once a game result is obtained in which vehicles on L2 become {the leader}, we record the lane-change cost of vehicles at this time and compare the costs of the first two items.

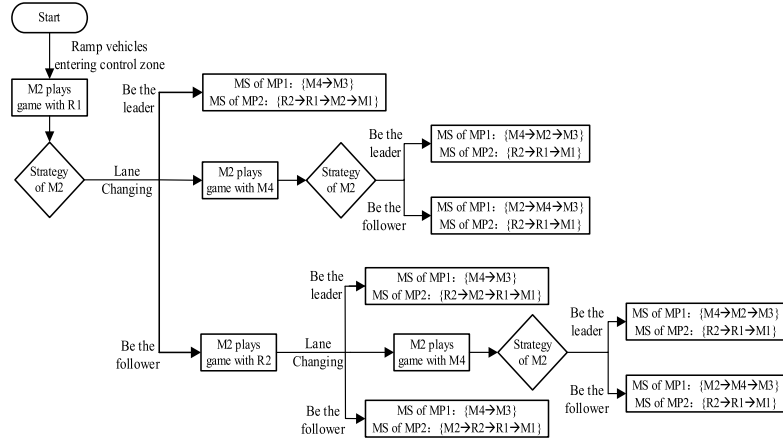


Fig. 3. Determining MS in multi-lane scenario.

Taking the Fig. 2 as an example, and combining it with the flowchart in Fig. 3, the possible merging results are as follow:

(1) M2 doesn't choose lane-changing strategy. When the game result between M2 and R1 is that M2 becomes the leader, the MS of MP2 is $\{R2 \rightarrow R1 \rightarrow M2 \rightarrow M1\}$. Otherwise, M2 will continue to play with R2. If M2 becomes the leader, then the MS of MP2 is $\{R2 \rightarrow M2 \rightarrow R1 \rightarrow M1\}$. If M2 becomes the follower, then the MS of MP2 is $\{M2 \rightarrow R2 \rightarrow R1 \rightarrow M1\}$. The MS of MP1 is the FIFO sequence on L1.

(2) M2 chooses the lane-changing strategy. The MS of MP2 is fixed; that is, the MS of MP2 is $\{R2 \rightarrow R1 \rightarrow M1\}$. Meanwhile, M2 primarily interacts with the vehicles on L1. Since M3 is the first vehicle on L1, M2 only needs play game with M4. If the game result indicates that M2 becomes the leader, then the MS result of MP1 is $\{M4 \rightarrow M2 \rightarrow M3\}$. Otherwise, the MS is $\{M2 \rightarrow M4 \rightarrow M3\}$. In addition, if there are vehicles behind M4 entering the control area, M2 will choose whether to continue the game with the new vehicles according to the game demand, to determine the final MS. Similarly, if vehicles remain behind M2, the steps in (1) will be repeated if it chooses not to change lanes in the game process, and the steps in (2) will be repeated if they choose to change lanes.

Once the vehicle enters the control area, it is regarded as a gameplayer by the central controller. The MS in MP2 is the main problem to be solved by the central controller, and the MS in MP1 is primarily determined by the game when the vehicle changes lanes from L2. Therefore, the cost of ramp vehicles is $J_R = J_{lon}$, the vehicle cost on L2 is $J_{L2} = J_{lon} + A J_{lat}$, and the vehicle cost on L1 is $J_{L1} = J_{lon}$. When the vehicle on L2 selects a lane-changing action, $A=1$ and J_{L1} participates in the game calculation; otherwise, $A=0$ and vehicles on L1 follow the FIFO sequence. According to the vehicle cost function constructed above, the cost values of subsets $\emptyset, \{1\}, \{1, 2\}, \dots, N$ in the control area can be obtained as follows:

$$\begin{cases} J(\emptyset) = 0 \\ J(\{1\}) = J_{v_1} \\ J(\{1, 2\}) = J_{v_1} + J_{v_2} \\ \dots \\ J(N) = J_{v_1} + J_{v_2} + \dots + J_{v_N} \end{cases} \quad (5)$$

Under the cooperative game, the MS decision-making problem of CAVs at the merging point can be expressed as

$$U^* = \arg \min \sum_{i=1}^N J_{v_i} \quad (6)$$

$$U^* = [u_{v_1}^*, \dots, u_{v_i}^*, \dots, u_{v_N}^*]^T \quad (7)$$

where U^* represents the optimal decision result of the N -vehicle CAVS game and $u_{v_i}^*$ represents the optimal result of vehicle i under pairwise game.

B. Solution Approach Based on Pontryagins Principle

The central controller can solve the MS of vehicles at the merging point through the cooperative game mentioned above. Then, depending on the initial and final states of the vehicle traffic control area, the central controller uses optimal control theory to plan and control the vehicle trajectory. This problem can be solved by the *Pontryagin maximum principle*. For the cost function and state equation of vehicles entering the control area, we introduce the co-state variable $\lambda = [\lambda_1, \lambda_2, \lambda_3]$ to establish and solve the Hamiltonian function for the longitudinal and lateral costs, respectively:

$$H = L(\mathbf{x}_i(t), \mathbf{u}_i(t), t) + \lambda^T f(\mathbf{x}_i(t), \mathbf{u}_i(t), t) \quad (8)$$

(1) Longitudinal Hamiltonian solution:

$$\begin{aligned} H_{log} = & \frac{1}{2} \omega_1 (v_x - v_{des})^2 + \frac{1}{2} \omega_2 a_x^2 + \frac{1}{2} \omega_3 u_x^2 \\ & + \lambda_{log1} v_x + \lambda_{log2} a_x + \lambda_{log3} u_x \end{aligned} \quad (9)$$

Then, we obtain the longitudinal co-state equations as

$$\dot{\lambda}_{log1} = -\frac{\partial H_{log}}{\partial x} = 0 \quad (10)$$

$$\dot{\lambda}_{log2} = -\frac{\partial H_{log}}{\partial v_x} = -\omega_1 (v_x - v_{des}) - \lambda_1 \quad (11)$$

$$\dot{\lambda}_{log3} = -\frac{\partial H_{log}}{\partial a_x} = -\omega_2 a_x - \lambda_2 \quad (12)$$

and the control equation is

$$\frac{\partial H_{log}}{\partial u_x} = \omega_3 u_x + \lambda_{log3} = 0 \quad (13)$$

By solving the above differential equation, the motion state of the vehicle in the control area can be obtained as

$$x = c_1 e^{r_1 t} + c_2 e^{r_2 t} + c_3 e^{r_3 t} + c_4 e^{r_4 t} + \left(v_{des} - \frac{c_5}{\omega_1} \right) t + \frac{c_6}{\omega_1} \quad (14)$$

$$v_x = c_1 r_1 e^{r_1 t} + c_2 r_2 e^{r_2 t} + c_3 r_3 e^{r_3 t} + c_4 r_4 e^{r_4 t} + \left(v_{des} - \frac{c_5}{\omega_1} \right) \quad (15)$$

$$a_x = c_1 r_1^2 e^{r_1 t} + c_2 r_2^2 e^{r_2 t} + c_3 r_3^2 e^{r_3 t} + c_4 r_4^2 e^{r_4 t} \quad (16)$$

$$u_x = c_1 r_1^3 e^{r_1 t} + c_2 r_2^3 e^{r_2 t} + c_3 r_3^3 e^{r_3 t} + c_4 r_4^3 e^{r_4 t} \quad (17)$$

where r_1, r_2, r_3 and r_4 are shown in Eq. (18)

$$\begin{cases} r_1 = -\left(\frac{\omega_2 + (\omega_2^2 - 4\omega_1\omega_3)^{1/2}}{2\omega_3}\right)^{1/2} \\ r_2 = \left(\frac{\omega_2 - (\omega_2^2 - 4\omega_1\omega_3)^{1/2}}{2\omega_3}\right)^{1/2} \\ r_3 = -\left(\frac{\omega_2 - (\omega_2^2 - 4\omega_1\omega_3)^{1/2}}{2\omega_3}\right)^{1/2} \\ r_4 = \left(\frac{\omega_2 + (\omega_2^2 - 4\omega_1\omega_3)^{1/2}}{2\omega_3}\right)^{1/2} \end{cases} \quad (18)$$

By analyzing the initial and final states, we set $x(t_0) = 0$ and $x(t_f) = L$, where L is the length of the control area; $v_x(t_0)$ and $a_x(t_0)$ depend on the initial state of the vehicle entering the control area; thus, we obtain

$$\begin{bmatrix} x(t_0) \\ v_x(t_0) \\ a_x(t_0) \\ x(t_f) \\ v_x(t_f) \\ a_x(t_f) \end{bmatrix} = R_{log} \begin{bmatrix} c_1 \\ c_2 \\ c_3 \\ c_4 \\ c_5 \\ c_6 \end{bmatrix} + \begin{bmatrix} v_{des}t_0 \\ v_{des} \\ 0 \\ v_{des}t_f \\ v_{des} \\ 0 \end{bmatrix} \quad (19)$$

And R_{log} is solved in Eq. (20),

$$R_{log} = \begin{bmatrix} e^{r_1 t_0} & e^{r_2 t_0} & e^{r_1 t_0} & e^{r_4 t_0} & -\frac{t_0}{w_1} & \frac{1}{w_1} \\ r_1 e^{r_1 t_0} & r_2 e^{r_2 t_0} & r_3 e^{r_1 t_0} & r_4 e^{r_4 t_0} & -\frac{1}{w_1} & 0 \\ r_1^2 e^{r_1 t_0} & r_2^2 e^{r_2 t_0} & r_3^2 e^{r_1 t_0} & r_4^2 e^{r_4 t_0} & 0 & 0 \\ e^{r_1 t_f} & e^{r_2 t_f} & e^{r_1 t_f} & e^{r_4 t_f} & -\frac{t_f}{w_1} & \frac{1}{w_1} \\ r_1 e^{r_1 t_f} & r_2 e^{r_2 t_f} & r_3 e^{r_1 t_f} & r_4 e^{r_4 t_f} & -\frac{1}{w_1} & 0 \\ r_1^2 e^{r_1 t_f} & r_2^2 e^{r_2 t_f} & r_3^2 e^{r_1 t_f} & r_4^2 e^{r_4 t_f} & 0 & 0 \end{bmatrix} \quad (20)$$

Therefore, we can obtain the constant vector as

$$\begin{bmatrix} c_1 \\ c_2 \\ c_3 \\ c_4 \\ c_5 \\ c_6 \end{bmatrix} = R_{log}^{-1} \left(\begin{bmatrix} x(t_0) \\ v_x(t_0) \\ a_x(t_0) \\ x(t_f) \\ v_x(t_f) \\ a_x(t_f) \end{bmatrix} - \begin{bmatrix} v_{des}t_0 \\ v_{des} \\ 0 \\ v_{des}t_f \\ v_{des} \\ 0 \end{bmatrix} \right) \quad (21)$$

The longitudinal analytic solution of the vehicle with respect to the position, velocity, acceleration, and jerk can be obtained by solving for the constant vector.

(2) Lateral Hamiltonian solution:

$$H_{lat} = \frac{1}{2} u_y^2 + \lambda_{lat1} v_y + \lambda_{lat2} a_y + \lambda_{lat3} u_y \quad (22)$$

The solution of lateral control is completely consistent with the longitudinal control. Relevant equations are as follows:

$$\dot{\lambda}_{lat1} = -\frac{\partial H_{lat}}{\partial y} = 0 \quad (23)$$

$$\dot{\lambda}_{lat2} = -\frac{\partial H_{lat}}{\partial v_y} = -\lambda_{lat1} \quad (24)$$

$$\dot{\lambda}_{lat3} = -\frac{\partial H_{lat}}{\partial a_y} = -\lambda_{lat2} \quad (25)$$

$$\frac{\partial H_{lat}}{\partial u_y} = u_y + \lambda_{lat3} = 0 \quad (26)$$

By solving the above differential equation, the motion state of vehicles during lane changes can be obtained as

$$y = -\frac{1}{120} c_7 t^5 - \frac{1}{24} c_8 t^4 - \frac{1}{6} c_9 t^3 - \frac{1}{2} c_{10} t^2 - c_{11} t - c_{12} \quad (27)$$

$$v_y = -\frac{1}{24} c_7 t^4 - \frac{1}{6} c_8 t^3 - \frac{1}{2} c_9 t^2 - c_{10} t - c_{11} \quad (28)$$

$$a_y = -\frac{1}{6} c_7 t^3 - \frac{1}{2} c_8 t^2 - c_9 t - c_{10} \quad (29)$$

$$u_y = -\frac{1}{2} c_7 t^2 - c_8 t - c_9 \quad (30)$$

Because the lateral cost is generated by vehicle lane changing, its initial and final state is $y(t_1) = 0, y(t_{LC}) = D$, where D is the lane width (generally 3.75 m). $v_y(t_1), a_y(t_1), v_y(t_{LC}),$ and $a_y(t_{LC})$ are the initial velocity, initial acceleration, final velocity, and final acceleration, respectively. To ensure safe lane changes, the above four values are all zero; thus, the following equation is obtained:

$$\begin{bmatrix} y(t_1) \\ v_y(t_1) \\ a_y(t_1) \\ y(t_{LC}) \\ v_y(t_{LC}) \\ a_y(t_{LC}) \end{bmatrix} = R_{lat} \begin{bmatrix} c_7 \\ c_8 \\ c_9 \\ c_{10} \\ c_{11} \\ c_{12} \end{bmatrix} \quad (31)$$

where

$$R_{lat} = \begin{bmatrix} -\frac{t_1^5}{120} & -\frac{t_1^4}{24} & -\frac{t_1^3}{6} & -\frac{t_1^2}{2} & -t_1 & -1 \\ -\frac{t_1^4}{24} & -\frac{t_1^3}{6} & -\frac{t_1^2}{2} & -t_1 & -1 & 0 \\ -\frac{t_1^3}{6} & -\frac{t_1^2}{2} & -t_1 & -1 & 0 & 0 \\ -\frac{t_{LC}^5}{120} & -\frac{t_{LC}^4}{24} & -\frac{t_{LC}^3}{6} & -\frac{t_{LC}^2}{2} & -t_{LC} & -1 \\ -\frac{t_{LC}^4}{24} & -\frac{t_{LC}^3}{6} & -\frac{t_{LC}^2}{2} & -t_{LC} & -1 & 0 \\ -\frac{t_{LC}^3}{6} & -\frac{t_{LC}^2}{2} & -t_{LC} & -1 & 0 & 0 \end{bmatrix} \quad (32)$$

TABLE II
WORKING CONDITION PARAMETERS

Parameter	Value
t_0	2 [s]
t_f	15 [s]
L	280 [m]
v_0	22 [m/s]
v_f	25 [m/s]
v_{des}	25 [m/s]
a_0	0
a_f	0

Therefore, the lateral constant vector is

$$\begin{bmatrix} c_7 \\ c_8 \\ c_9 \\ c_{10} \\ c_{11} \\ c_{12} \end{bmatrix} = R_{lat}^{-1} \begin{bmatrix} y(t_1) \\ v_y(t_1) \\ a_y(t_1) \\ y(t_{LC}) \\ v_y(t_{LC}) \\ a_y(t_{LC}) \end{bmatrix} \quad (33)$$

Similarly, by solving the constant vector of the lateral cost, the lateral cost of vehicles on L2 can be obtained when they choose a lane-changing strategy.

Finally, the analytic solution of the position, velocity, and acceleration of each vehicle can be obtained using a constant vector. After solving for the optimal u^* and determining the corresponding strategy of the minimum cost J^* , the Pareto efficiency of the two-player game can be obtained from the cost matrix. When the vehicle enters the control area, the central controller determines the optimal MS. From the vehicle status collected at each sampling time, the optimal trajectory of each vehicle is updated to manage interference until the MS is completed.

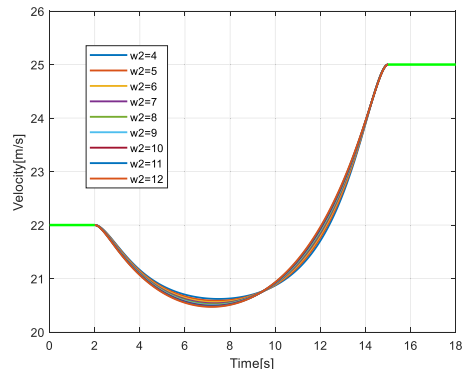
IV. SIMULATION

A. Weight Analysis

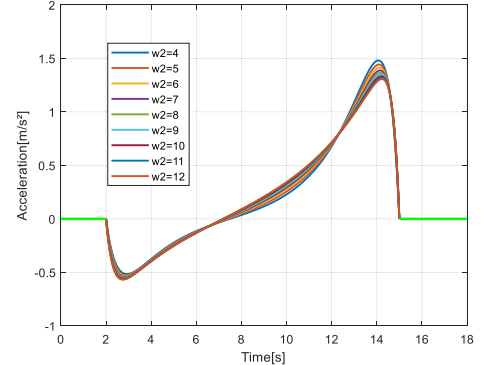
The longitudinal cost function of the CAVS includes the weights ω_1 , ω_2 , and ω_3 , affecting the driving efficiency, fuel consumption and ride comfort, respectively. The calculation value of cost is directly related to the weight value. At same time, these values also affect the velocity and acceleration of vehicles. Therefore, a reasonable weight is conducive to system stability. It is worth noting that when $\omega_2^2 \geq \omega_1\omega_3$, the solution to the state of motion equation is meaningful. When $\omega_2^2 = \omega_1\omega_3$, the solution of the constant matrix exhibits a singular value; therefore, we must satisfy $\omega_2^2 > \omega_1\omega_3$. Hence, for the conditions listed in Table II, the recommended values of ω_1 , ω_2 , and ω_3 are discussed here.

Because ω_2 depends on the values of ω_1 and ω_3 , to determine the impact of ω_2 on vehicle velocity and acceleration, we first fixed $\omega_1 = \omega_3 = 1$ and varied ω_2 from its critical value, to observe the change in vehicle's velocity and acceleration. The results are shown in Fig. 4.

From the above figures, we can see that ω_2 has little impact on the velocity and acceleration under the above working conditions. However, ω_2 determines the cost of vehicle



(a) Optimal velocity results.



(b) Optimal acceleration results.

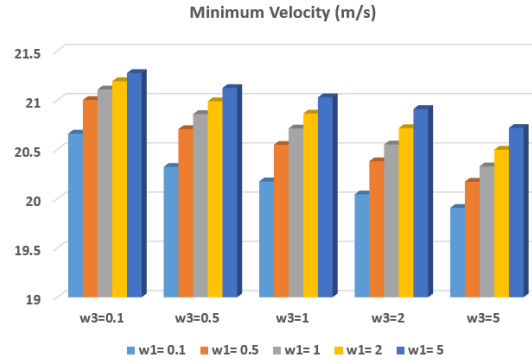
Fig. 4. Optimal results for (a) velocity and (b) acceleration under different ω_2 .

acceleration in the control area; hence, to minimize this cost, we suggest setting ω_2 is slightly greater than the critical value.

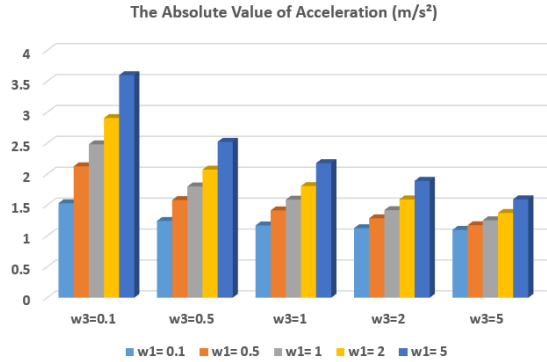
To further determine the values of ω_1 and ω_3 , we take the above working conditions as an example and make ω_2 slightly greater than the critical value. Then, we discuss the impact of different combinations of ω_1 and ω_3 upon vehicle's velocity, acceleration, and jerk. The central controller determines the initial and final states for vehicles entering and leaving the control area; that is, when determining the travel time of vehicles, the average velocity of vehicles is unchanged. Therefore, in this section, the lowest velocity of the vehicle in the control area was used to reflect the vehicle driving efficiency. The results are shown in Fig. 5.

In the above results, the smaller the ω_1 , the larger the ω_3 , and the smaller and more variable the acceleration and jerk of the vehicle. Under this working condition, and excessively small value of ω_3 will produce a sizeable jerk and thereby fail to meet the actual driving demand. Therefore, the value of ω_3 should be as large as possible. However, when $\omega_3 = 5$, the smaller the value of ω_1 , the less obvious the change in acceleration and jerk; furthermore, the minimum velocity of the vehicle in the control area will be reduced, thereby reducing the driving efficiency.

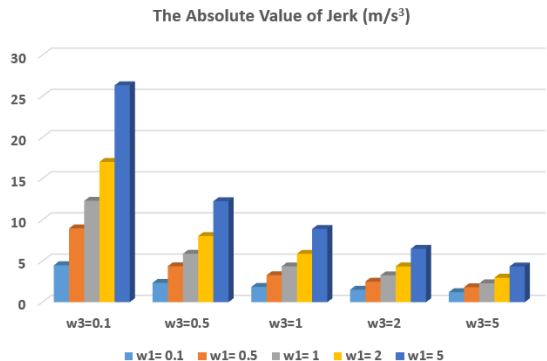
Therefore, to consider the driving efficiency of the vehicle alongside the fuel economy and actual driving comfort, we suggest that ω_1 is taken as 1, and ω_3 is taken as 5; the value of ω_2 should be slightly larger than the critical value, and we set $\omega_2 = 2\sqrt{5} + 0.1$.



(a) Optimal minimum velocity result.



(b) Optimal acceleration results.



(c) Optimal jerk result.

Fig. 5. Optimal results of minimum velocity, acceleration, and jerk under different ω_1 and ω_3 combinations.

B. Merging Case Study in Multi-Lane Environment Based on Cooperative Game

To verify the effectiveness of the model, we carried out the simulation of working conditions under the equipment of CPU: i5 7400, Operating frequency: 3.0 GHz, RAM: 16GB. The detailed simulation conditions are set as follows: 9 vehicles on L1, 9 vehicles on L2, and 8 vehicles on the ramp. Assuming that L1/L2 vehicles and ramp vehicles enter the control area at random velocities from 20 to 22m/s and 16 to 18m/s, respectively. The initial acceleration of all vehicles is between [0, 0.3] m/s^2 . By analyzing the ramp length in the real dataset, the length of the control area L is 280 m, safe headway $T_s=2\text{s}$ [33]. In order to simplify the game, we make the desired velocity of all vehicles equal the terminal velocity (in fact, the desired velocity of the vehicle depends to a large extent on the driver's subjective wishes). Depending on the time sequence

TABLE III
TIME AT WHICH VEHICLES IN DIFFERENT LANES
ENTER THE CONTROL AREA

L1		L2		Ramp	
Enter ID	$t_0[\text{s}]$	Enter ID	$t_0[\text{s}]$	Enter ID	$t_0[\text{s}]$
2	0.8	1	0	3	2.2
5	3.6	4	2.3	7	5.5
9	7	6	4.7	10	8.2
12	10.1	8	6.7	13	10.5
14	12.6	11	9.8	16	13.8
17	15.6	15	13.1	19	16.9
20	17.9	18	16.4	22	20.2
23	21.3	21	19	25	22.6
26	24.8	24	21.7		

of vehicles entering the control area, each vehicle is assigned an Enter ID, in which No.2 on L1 and No.1 on L2 are the first vehicles on the two lanes; that is, the states of the two vehicles arriving at the merging point are known, and they do not participate in the game. The times when other vehicles entering the control area are shown in Table III.

The multi-vehicle game cost matrix is presented in Table IV. Under the cooperative game, the central controller can calculate the game cost of vehicles in real time and determine the MS in which vehicles pass through MP1 and MP2. The position, velocity, and acceleration profile of each vehicle can then be calculated via optimal control, as shown in Figs. 6–10. Figs. 6 and 7 show the vehicles passing through MP1 and MP2.

Table V shows the game strategies and costs for vehicles on L1 and L2. And whether vehicles on L2 changing lane depends on whether it can pass through MP1 as the “leader” and which of the three strategies is lowest. Therefore, by combining Tables IV and V, it can be concluded that the MS of MP1 is 2-5-6-8-9-12-14-17-18-20-23-24-26, as shown in Fig. 7.

The space-time trajectory distribution of the multi-vehicle in Fig. 8 shows that vehicles entering the control area from L2 do not necessarily merge in MP2. To fully utilize the lane, it is also possible to adopt lane-changing strategies during the game. Meanwhile, the “first in” of vehicles does not entail “first out”. For example, NO.4 on L2 arrives at MP2 earlier than NO.3 on the ramp, which indicates that the cooperative game fully ensures the unified interests of vehicles during merging.

Fig. 9 shows that ramp vehicles continue to accelerate during the merging to reach the same velocity as the vehicles on the mainline. In addition, the minimum velocity of all vehicles exceeds 16 m/s, which indicates that stop-go does not occur during the merging process, effectively ensuring smooth passage in the control area. Fig. 10 shows that under the proposed optimization strategy, the vehicle acceleration is maintained in the range [-1, 2] m/s^2 , ensuring comfortable and economical driving.

Significantly, based on the above simulation, the maximum calculation time of each two-person game is 0.57s, and the average calculation time is 0.46s. Compared with the distributed algorithm, the execution efficiency has some defects,

TABLE IV
GAME COST MATRIX OF L1 AND L2 VEHICLES

Strategy	(U _{4L,3F})	(U _{4F,3L})	(U _{4LC,3L})	(U _{6L,3F})	(U _{6F,3L})	(U _{6LC,3L})
Cost	32.4	49.7	35.1	76.8	47.1	34
Strategy	(U _{8L,7F})	(U _{8F,7L})	(U _{8LC,7L})	(U _{11L,10F})	(U _{11F,10L})	(U _{11LC,10L})
Cost	47.9	34.9	23.3	85.2	27.7	43.7
Strategy	(U _{11L,13F})	(U _{11F,13L})	(U _{11LC,13L})	(U _{15L,13F})	(U _{15F,13L})	(U _{15LC,13L})
Cost	27.2	85.9	62.7	84.4	35	55.3
Strategy	(U _{15L,16F})	(U _{15F,16L})	(U _{15LC,16L})	(U _{18L,16F})	(U _{18F,16L})	(U _{18LC,16L})
Cost	44.8	85	59.3	83	57.9	44
Strategy	(U _{21L,19F})	(U _{21F,19L})	(U _{21LC,19L})	(U _{21L,22F})	(U _{21F,22L})	(U _{21LC,22L})
Cost	67.9	32.7	54.8	40.8	94.5	67.2
Strategy	(U _{24L,22F})	(U _{24F,22L})	(U _{24LC,22L})			
Cost	72.4	69.9	47.2			

TABLE V
GAME COST MATRIX OF L2 AND RAMP VEHICLES

Strategy	(U _{5L,4F})	(U _{5F,4L})	(U _{5L,6F})	(U _{5F,6L})	(U _{9L,6F})	(U _{9F,6L})
Cost	55.3	27.7	12.7	88.1	159.4	9.1
Strategy	(U _{9L,8F})	(U _{9F,8L})	(U _{9L,11F})	(U _{9F,11L})	(U _{12L,11F})	(U _{12F,11L})
Cost	44.9	34.9	46.3	100.3	76.7	72.9
Strategy	(U _{12L,15F})	(U _{12F,15L})	(U _{14L,15F})	(U _{14F,15L})	(U _{17L,15F})	(U _{17F,15L})
Cost	16.8	192.9	32.6	54.1	90.1	48.2
Strategy	(U _{17L,18F})	(U _{17F,18L})	(U _{20L,18F})	(U _{20F,18L})	(U _{20L,21F})	(U _{20F,21L})
Cost	15.3	76.2	59.4	22	47.3	71
Strategy	(U _{23L,21F})	(U _{23F,21L})	(U _{23L,24F})	(U _{23F,24L})	(U _{26L,24F})	(U _{26F,24L})
Cost	94.7	56.9	23.2	40.2	152.7	20.6

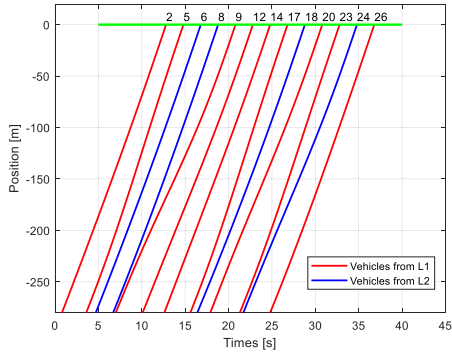


Fig. 6. Position trajectory of vehicles passing MP1.

but it still shows that the algorithm we proposed has certain real-time in the centralized decision-making control, and the efficiency will be further improved when facing more efficient vehicle-road collaborative computing equipment.

In order to further explain the traffic efficiency and fuel economy of vehicles in the merging area, we compared the proposed algorithm, the algorithm in literature [42] and the FIFO algorithm. According to our summary of the existing literature, there are few merging models for multi-lane centralized control at present, so the two algorithms in above comparison are applied in single mainline merging scenario. However, the subject and object of our comparison are the

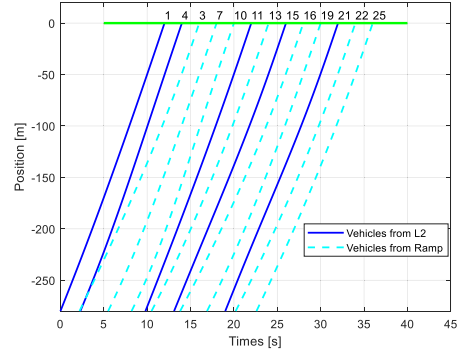


Fig. 7. Position trajectory of vehicles passing MP2.

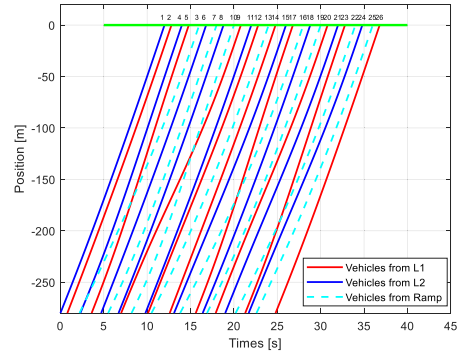


Fig. 8. Space time trajectory of all vehicles.

same, that is, 17 vehicles on L2 and ramp (as shown in the simulation above) have the same initial conditions and terminal conditions. Since the VT Micro model [43] has great accuracy and stability on estimating vehicle fuel consumption, we use this model to calculate vehicle fuel consumption. The results are shown in Figs 11 and 12.

Fig. 11 shows a comparison of the fuel consumption and average velocities of the 17 vehicles under the above three algorithms. In the single lane scenario, when the game merging strategy in [42] was consistent with the FIFO merging strategy, the average velocities and fuel consumptions of the vehicles

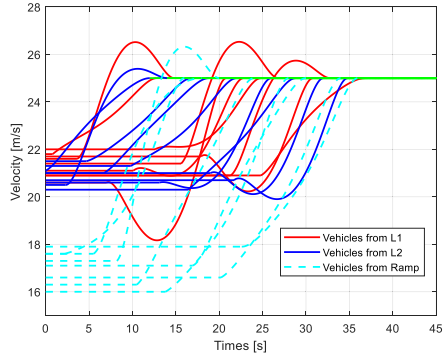


Fig. 9. Velocity profiles of all vehicles.

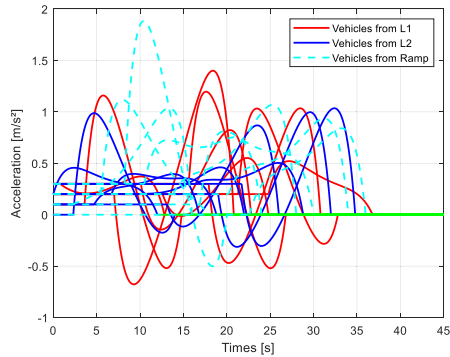


Fig. 10. Acceleration profiles of all vehicles.

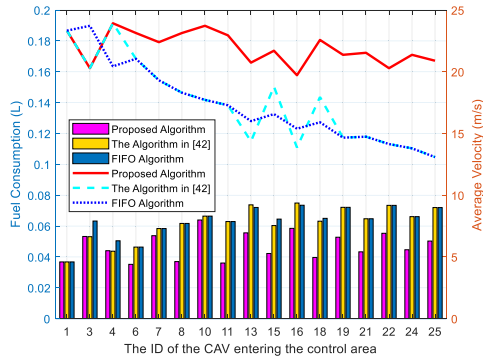


Fig. 11. Vehicles' fuel consumption and average velocity under three models.

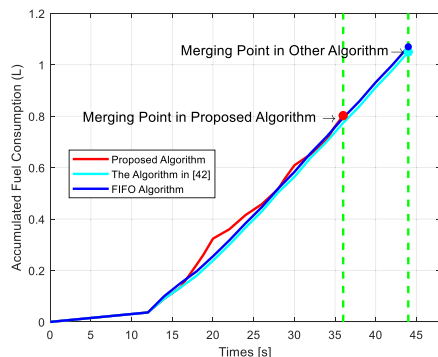


Fig. 12. Accumulated fuel consumption in control area under three algorithms.

were equal, and the difference was minimal when the strategies differed. However, the multi-lane game merging strategy in this study can effectively reduce vehicle fuel consumption



Fig. 13. Visualization of vehicles entering the control area.

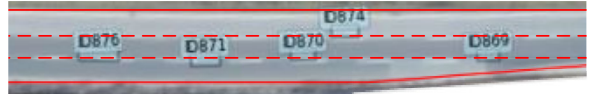


Fig. 14. Visualization of partial vehicles arriving at MP.

and considerably improve the average velocity of the vehicles, because of the design of the efficiency cost function.

Fig. 12 shows the cumulative fuel consumption of the vehicles arriving at the merging point through the control area under the three models. The dotted green line and the ordinate denote the total travel time and cumulative fuel consumption, respectively, of the vehicles arriving at the merging point. Since the strategy of the first vehicle under the three algorithms is the same, the initial fuel consumption is the same. However, with the obvious changes in decision-making, the total travel time and fuel consumption at the merging point have changed greatly. Due to the benefits of multi-lane, vehicles entering L2 can effectively reduce driving time and fuel consumption under the lane change strategy. Specifically, the model in this study can improve the average velocity by 25.79% and reduce the fuel consumption by 23.6% compared to the single main lane game merging strategy model proposed in [42]. Compared with the single main lane FIFO merging strategy model, it can increase the average velocity by 26.3% and reduce fuel consumption by 25.01%. Simultaneously, since there is only one merging point, the total travel time of the algorithm in [42] and the FIFO algorithm are the same. And the strategy in this study can reduce the total travel time of ramp vehicles to the merging point by 18.2%, because vehicles on L2 can change lanes.

C. Comparative Experiment With ExID Dataset

To further verify the applicability of the model in this study, we conducted a simulation comparison according to the driving conditions of real vehicles in the ExID dataset [44]. The ExID dataset is a ramp scene comprising seven typical road sections in Germany, as recorded and tracked by the German FKA team using unmanned aerial vehicles. Its rich data format and excellent data accuracy make it suitable for research into the decision planning and testing of autonomous vehicles.

We selected a merging scenario in file-75 under the Aachen Laurensberg section of the ExID. By analyzing the openDrive map, the length of the control area is still set as 280m, and we assumed that all vehicles are CAVs. The velocity of this road section is high, and the headway of adjacent vehicles is small. In order to better compare with ExID in decision-making and optimization. We set T_s to 1s by referring to the results of the dataset. At last, we extract the initial and final states of the

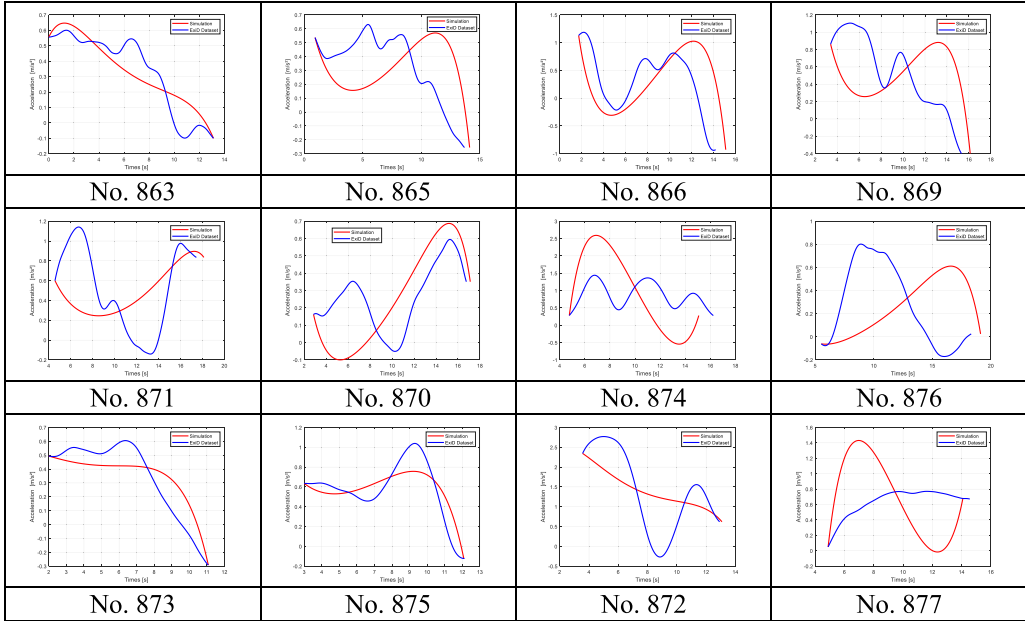


Fig. 15. Acceleration comparison between simulation and EixD.

TABLE VI
GAME COST MATRIX OF L2 AND RAMP VEHICLES

Strategy Cost	(U _{870L,865F})	(U _{870F,865L})	(U _{870LC,865L})
	72.99	20.01	66.31
Strategy Cost	(U _{870L,866F})	(U _{870F,866L})	(U _{870LC,866L})
	53.85	22.93	78.69
Strategy Cost	(U _{870L,869F})	(U _{870F,869L})	(U _{870LC,869L})
	40.34	25.36	75.55
Strategy Cost	(U _{870L,871F})	(U _{870F,871L})	(U _{870LC,871L})
	25.35	33.42	70.06
Strategy Cost	(U _{874L,871F})	(U _{874F,871L})	(U _{874LC,871L})
	114.89	138.9	63.79

merged vehicles to validate the proposed multi-lane merging algorithm.

According to the ExID visualization interface, the scenarios for the 12 vehicles entering the control area is as shown in Fig. 13. Vehicles 873, 875, 872, and 877 were located on L1; Vehicles 870, 874, and 876 were located on L2; Vehicles 863, 865, 866, 869, and 871 were located on the ramp; and Vehicle 873 was the first vehicle on L1 (i.e., the first vehicle to pass through MP1). Similarly, Vehicle 863 was the first vehicle on L2 and ramp (i.e., the first vehicle to pass through MP2). Because the starting frame of Vehicle 863 entering the control area was smallest, the time at which the vehicle entered the control area was defined as the simulation starting point (i.e., $t_0 = 0$), in which the time t_{f1} of the first vehicle (873) passing through the MP1 was 11.08 s, and the time t_{f2} of the first vehicle (863) passing through MP2 was 13.12 s.

After applying the optimal multi-lane merging strategy algorithm using the cooperative game in this study, the game cost matrix of 12 vehicles was obtained as shown in Tables VI and VII, where the first vehicle does not participate in the game.

Table VI shows the game cost matrix between L2 and ramp vehicles on MP2, and Table VII shows the game results

TABLE VII
GAME COST MATRIX OF L1 AND L2 VEHICLES

Strategy Cost	(U _{870L,875F})	(U _{870F,875L})	(U _{870L,872F})	(U _{870F,872L})
	450.93	164.57	235.55	91.61
Strategy Cost	(U _{870L,877F})	(U _{870F,877L})	(U _{874L,877F})	(U _{874F,877L})
	28.2	80.91	167.98	56.94

between L2 and L1 vehicles when choosing lane-changing strategies. Because the final game result of MP1 was Vehicle 874 lane-changing to L1, Vehicle 871 arrived at MP1 first. To reduce unnecessary lane-changing, Vehicle 876 did not need to participate in the game. Therefore, the final MS of MP1 was 873-875-872-877-874, and the MS of MP2 was 863-865-866-869-870-871-876.

Fig. 14 shows the visualization interface for the vehicles arriving at the merging point. At this time, Vehicles 873, 875, 872, and 877 on L1 passed through MP1, and Vehicle 874 completed the lane change. Among the L2 and ramp vehicles, Vehicles 876, 871, and 870 also passed MP2. That is, the simulation by our model was consistent with the real merging situation of vehicles in the ExID dataset, which indicates that the algorithm model in this study has practical significance. Thus, to further illustrate the advantages of the optimal control in this study under the condition that the simulation strategy is consistent with the real strategy, we compared the acceleration change and fuel consumption of vehicles in the simulation test and real dataset, as shown in Figs. 15 and 16.

In Fig. 15, the blue line represents the acceleration trajectory of the ExID dataset, the red line represents the simulation results under optimal control, and the abscissa of each subgraph denotes the vehicle ID. Under the same merging strategy, the optimal control optimization-based acceleration in this study was smoother and more stable, without severe jitter, effectively ensuring the comfort of the vehicle. Even though the acceleration changes for certain vehicles were

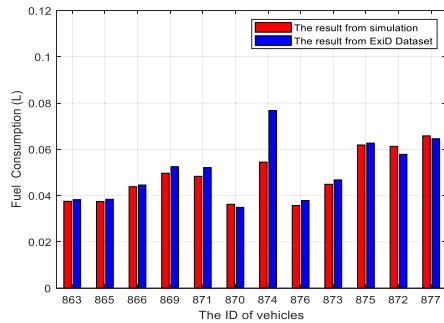


Fig. 16. Comparison of fuel consumption between simulation and ExiD dataset.

markedly different, we found that the average acceleration of the simulation was very close to the average acceleration of ExiD, and the maximum difference was no more than 0.04 m/s^2 . The acceleration of the simulation data and ExiD reached the same terminal value at different time, which is caused by the value of T_s in the game.

Fig. 16 presents a comparison between the simulated fuel consumption of the above 12 vehicles under the optimal control strategy and the fuel consumption of ExiD. The fuel consumption derived from optimal control was generally lower than that of the vehicles in ExiD. The overall fuel consumption of vehicles was 4.95% lower than that in the real environment, which shows that the optimization method in this study has a certain practical significance, and that it can achieve good results in the simulation test with respect to the real data.

The comparison of MS and optimization results between the proposed algorithm and the real dataset, it is proved that our model can reflect the humanoid nature of the game to a certain extent in the multi-lane merging scene. Under the condition of consistent decision, the control optimization model can create more gentle acceleration change and effectively reduce fuel consumption.

V. CONCLUSION

In this study, we solved the coordination MS problem of ramp vehicles using cooperative game theory. First, we constructed a multi-lane merging area scenario to allow vehicles on the mainline to opt to change lanes when merging with ramp vehicles. Second, we designed a multi-objective cost function including vehicle driving efficiency, comfort, and fuel consumption, and we analyzed the vehicle cost under different game strategies. Finally, by using the *Pontryagins principle*, we solved the optimal coordinated trajectories of vehicles under the optimal combination strategy. The simulation results show that the proposed model can effectively complete the MS for vehicles. Compared with other model algorithms, the proposed model can significantly reduce vehicle fuel consumption, improve efficiency, reduce the merging travel time of ramp vehicles, and improve comfort. In addition, by comparing the driving conditions with the real dataset, we show that our decision-making model has practical significance, can improve driving comfort, and can reduce vehicle fuel consumption when the simulation strategy is consistent with the actual strategy.

Our focus is to solve the MS problem of ramp vehicles in the full CAVS environment. So, there is no more consideration

for vehicle decision-making in the case of mixed connection. At the same time, the study on vehicle lateral control also needs to be further expanded. In the future work, we will first discuss and analyze the merging decision of the mixed state, aiming to solve the decision-making sequence of different vehicles through different game strategies. And lateral control research is carried out for mainline and on-ramp vehicles respectively.

REFERENCES

- [1] J. Zhu, S. Easa, and K. Gao, "Merging control strategies of connected and autonomous vehicles at freeway on-ramps: A comprehensive review," *J. Intell. Connected Vehicles*, vol. 5, no. 2, pp. 99–111, May 2022.
- [2] D. Hale et al., "Introduction of cooperative vehicle-to-infrastructure systems to improve speed harmonization," U.S. Dept. Transp., FHWA, Washington, DC, USA, 2016, pp. 23–36.
- [3] K. Raboy, J. Ma, E. Leslie, and F. Zhou, "A proof-of-concept field experiment on cooperative lane change maneuvers using a prototype connected automated vehicle testing platform," *J. Intell. Transp. Syst.*, vol. 25, pp. 77–92, Jan. 2021.
- [4] Y. Liu, Q. Zhang, C. Lyu, and Z. Liu, "Modelling the energy consumption of electric vehicles under uncertain and small data conditions," *Transp. Res. A, Policy Pract.*, vol. 154, pp. 313–328, Dec. 2021.
- [5] A. Ansariyari and M. Tahmasebi, "Investigating the effects of gradual deployment of market penetration rates (MPR) of connected vehicles on delay time and fuel consumption," *J. Intell. Connected Vehicles*, vol. 5, no. 3, pp. 188–198, Oct. 2022.
- [6] S. Fang, L. Yang, T. Wang, and S. Jing, "Trajectory planning method for mixed vehicles considering traffic stability and fuel consumption at the signalized intersection," *J. Adv. Transp.*, vol. 2020, pp. 1–10, Jan. 2020.
- [7] L. Xu, S. Jin, B. Li, and J. Wu, "Traffic signal coordination control for arterials with dedicated CAV lanes," *J. Intell. Connected Vehicles*, vol. 5, no. 2, pp. 72–87, May 2022.
- [8] H. Pei, S. Feng, Y. Zhang, and D. Yao, "A cooperative driving strategy for merging at on-ramps based on dynamic programming," *IEEE Trans. Veh. Technol.*, vol. 68, no. 12, pp. 11646–11656, Dec. 2019.
- [9] Y. Ito, M. A. S. Kamal, T. Yoshimura, and S. Azuma, "Coordination of connected vehicles on merging roads using pseudo-perturbation-based broadcast control," *IEEE Trans. Intell. Transp. Syst.*, vol. 20, no. 9, pp. 3496–3512, Sep. 2019.
- [10] J. Rios-Torres and A. A. Malikopoulos, "A survey on the coordination of connected and automated vehicles at intersections and merging at highway on-ramps," *IEEE Trans. Intell. Transp. Syst.*, vol. 18, no. 5, pp. 1066–1077, May 2017.
- [11] G. Schmidt and B. Posch, "A two-layer control scheme for merging of automated vehicles," in *Proc. 22nd IEEE Conf. Decis. Control*, Dec. 1983, pp. 495–500.
- [12] J. Rios-Torres and A. A. Malikopoulos, "Automated and cooperative vehicle merging at highway on-ramps," *IEEE Trans. Intell. Transp. Syst.*, vol. 18, no. 4, pp. 780–789, Apr. 2017.
- [13] W. Xiao and C. G. Cassandras, "Decentralized optimal merging control for connected and automated vehicles with safety constraint guarantees," *Automatica*, vol. 123, Jan. 2021, Art. no. 109333.
- [14] V. Milanes, J. Godoy, J. Villagra, and J. Perez, "Automated on-ramp merging system for congested traffic situations," *IEEE Trans. Intell. Transp. Syst.*, vol. 12, no. 2, pp. 500–508, Jun. 2011.
- [15] C. P. Huang, M. Jiang, and G. Chai, "Fuzzy control for ramp metering and variable velocity limitation of freeway," *J. Comput. Technol.*, vol. 20, no. 12, pp. 38–41, 2010.
- [16] M. Zhou, X. Qu, and S. Jin, "On the impact of cooperative autonomous vehicles in improving freeway merging: A modified intelligent driver model-based approach," *IEEE Trans. Intell. Transp. Syst.*, vol. 18, no. 6, pp. 1422–1428, Jun. 2017.
- [17] Y. Xue, C. Ding, B. Yu, and W. Wang, "A platoon-based hierarchical merging control for on-ramp vehicles under connected environment," *IEEE Trans. Intell. Transp. Syst.*, vol. 23, no. 11, pp. 21821–21832, Nov. 2022.
- [18] E. Beheshtabar and E. M. Alipour, "A rule based control algorithm for on-ramp merge with connected and automated vehicles," in *Proc. Int. Conf. Transp. Develop.*, Aug. 2020, pp. 303–316.

- [19] J. Ding, L. Li, H. Peng, and Y. Zhang, "A rule-based cooperative merging strategy for connected and automated vehicles," *IEEE Trans. Intell. Transp. Syst.*, vol. 21, no. 8, pp. 3436–3446, Aug. 2020.
- [20] H. Bi, W.-L. Shang, Y. Chen, and K. Wang, "Joint optimization for pedestrian, information and energy flows in emergency response systems with energy harvesting and energy sharing," *IEEE Trans. Intell. Transp. Syst.*, vol. 23, no. 11, pp. 22421–22435, Nov. 2022.
- [21] J. M. Tien, "Convergence to real-time decision making," *Frontiers Eng. Manag.*, vol. 7, no. 2, pp. 204–222, Jun. 2020.
- [22] X. Chen, Z. Wang, Q. Hua, W.-L. Shang, Q. Luo, and K. Yu, "AI-empowered speed extraction via port-like videos for vehicular trajectory analysis," *IEEE Trans. Intell. Transp. Syst.*, vol. 24, no. 4, pp. 4541–4552, Apr. 2023.
- [23] Y. Zhou, M. E. Cholette, A. Bhaskar, and E. Chung, "Optimal vehicle trajectory planning with control constraints and recursive implementation for automated on-ramp merging," *IEEE Trans. Intell. Transp. Syst.*, vol. 20, no. 9, pp. 3409–3420, Sep. 2019.
- [24] L. Xu, J. Lu, B. Ran, F. Yang, and J. Zhang, "Cooperative merging strategy for connected vehicles at highway on-ramps," *J. Transp. Eng., A Syst.*, vol. 145, no. 6, Jun. 2019, Art. no. 04019022.
- [25] W. Cao, M. Mukai, T. Kawabe, H. Nishira, and N. Fujiki, "Gap selection and path generation during merging maneuver of automobile using real-time optimization," *SICE J. Control, Meas., Syst. Integr.*, vol. 7, no. 4, pp. 227–236, Jul. 2014.
- [26] W. Cao, M. Mukai, T. Kawabe, H. Nishira, and N. Fujiki, "Cooperative vehicle path generation during merging using model predictive control with real-time optimization," *Control Eng. Pract.*, vol. 34, pp. 98–105, Jan. 2015.
- [27] S. Jing, F. Hui, X. Zhao, J. Rios-Torres, and A. J. Khattak, "Integrated longitudinal and lateral hierarchical control of cooperative merging of connected and automated vehicles at on-ramps," *IEEE Trans. Intell. Transp. Syst.*, vol. 23, no. 12, pp. 24248–24262, Dec. 2022.
- [28] S. Jing, X. Zhao, F. Hui, A. J. Khattak, and L. Yang, "Cooperative CAVs optimal trajectory planning for collision avoidance and merging in the weaving section," *Transportmetrica B, Transp. Dyn.*, vol. 9, no. 1, pp. 219–236, Jan. 2021.
- [29] I. A. Ntousakis, I. K. Nikолос, and M. Papageorgiou, "Optimal vehicle trajectory planning in the context of cooperative merging on highways," *Transp. Res. C, Emerg. Technol.*, vol. 71, pp. 464–488, Oct. 2016.
- [30] A. Sathyan, J. Ma, and K. Cohen, "Decentralized cooperative driving automation: A reinforcement learning framework using genetic fuzzy systems," *Transportmetrica B, Transp. Dyn.*, vol. 9, no. 1, pp. 775–797, Jan. 2021.
- [31] S. Karbalaei, O. A. Osman, and S. Ishak, "A dynamic adaptive algorithm for merging into platoons in connected automated environments," *IEEE Trans. Intell. Transp. Syst.*, vol. 21, no. 10, pp. 4111–4122, Oct. 2020.
- [32] J. Liu, W. Zhao, and C. Xu, "An efficient on-ramp merging strategy for connected and automated vehicles in multi-lane traffic," *IEEE Trans. Intell. Transp. Syst.*, vol. 23, no. 6, pp. 5056–5067, Jun. 2022.
- [33] A. Ji and D. Levinson, "A review of game theory models of lane changing," *Transportmetrica A, Transp. Sci.*, vol. 16, no. 3, pp. 1628–1647, Jan. 2020.
- [34] R. Chen and Z. Yang, "A cooperative merging strategy for connected and automated vehicles based on game theory with transferable utility," *IEEE Trans. Intell. Transp. Syst.*, vol. 23, no. 10, pp. 19213–19223, Oct. 2022.
- [35] Z. Liu et al., "Government regulation to promote coordinated emission reduction among enterprises in the green supply chain based on evolutionary game analysis," *Resour. Conservation Recycling*, vol. 182, Jul. 2022, Art. no. 106290.
- [36] H. X. Liu, W. Xin, Z. Adam, and X. Ban, "A game theoretical approach for modelling merging and yielding behaviour at freeway on-ramp sections," in *Proc. 17th Int. Symp. Transp. Traffic Theory*, 2007, pp. 197–211.
- [37] H. Yu, H. E. Tseng, and R. Langari, "A human-like game theory-based controller for automatic lane changing," *Transp. Res. C, Emerg. Technol.*, vol. 88, pp. 140–158, Mar. 2018.
- [38] H. Kita, "A merging-giveaway interaction model of cars in a merging section: A game theoretic analysis," *Transp. Res. A, Policy Pract.*, vol. 33, nos. 3–4, pp. 305–312, 2019.
- [39] C. Wei, Y. He, H. Tian, and Y. Lv, "Game theoretic merging behavior control for autonomous vehicle at highway on-ramp," *IEEE Trans. Intell. Transp. Syst.*, vol. 23, no. 11, pp. 21127–21136, Nov. 2022.
- [40] X. Liao et al., "Game theory-based ramp merging for mixed traffic with unity-SUMO co-simulation," *IEEE Trans. Syst., Man, Cybern. Syst.*, vol. 52, no. 9, pp. 5746–5757, Sep. 2022.
- [41] P. Hang, C. Lv, C. Huang, Y. Xing, and Z. Hu, "Cooperative decision making of connected automated vehicles at multi-lane merging zone: A coalitional game approach," *IEEE Trans. Intell. Transp. Syst.*, vol. 23, no. 4, pp. 3829–3841, Apr. 2022.
- [42] S. Jing, F. Hui, X. Zhao, J. Rios-Torres, and A. J. Khattak, "Cooperative game approach to optimal merging sequence and on-ramp merging control of connected and automated vehicles," *IEEE Trans. Intell. Transp. Syst.*, vol. 20, no. 11, pp. 4234–4244, Nov. 2019.
- [43] K. Ahn, H. Rakha, A. Trani, and M. van Aerde, "Estimating vehicle fuel consumption and emissions based on instantaneous speed and acceleration levels," *J. Transp. Eng.*, vol. 128, no. 2, pp. 182–190, 2002.
- [44] T. Moers, L. Vater, R. Krajewski, J. Bock, A. Zlocki, and L. Eckstein, "The exiD dataset: A real-world trajectory dataset of highly interactive highway scenarios in Germany," in *Proc. IEEE Intell. Vehicles Symp. (IV)*, Jun. 2022, pp. 958–964.

Lan Yang received the Ph.D. degree from Chang'an University, China, in 2013. Currently, she is an Associate Professor with the School of Information Engineering, Chang'an University. Her research interests include the cooperative eco-driving of CAVs, vehicle active safety technology, and vehicle behavior cognition.



Jiahao Zhan received the B.E. degree in electronic information engineering from Nanchang Hangkong University, Nanchang, China, in 2021. He is currently pursuing the M.Eng. degree in transportation engineering with Chang'an University, China. His research interests include decision-making and the control of automated vehicle.



Wen-Long Shang (Member, IEEE) received the Ph.D. degree from the Centre for Transport Studies, Department of Civil and Environmental Engineering, Imperial College London. He is currently an Honorary Senior Research Fellow with Imperial College London and a Lecturer with the College of Metropolitan Transportation, Beijing University of Technology. He has already published more than 60 academic papers in peer-reviewed top journals and conferences, and participated in the writing of a book *Big Data and Mobility as a Service* and a report for the Asian Development Bank Institute. He serves as the managing guest editor and a member of editorial board for many international academic journals. He is a reviewer of more than 60 journals and conferences. His research interests include intelligent transport systems, the emergency management of transport systems, energy conservation, the emission reduction of transport systems, traffic big data, and smart city.



Shan Fang received the B.S. degree in computer science from Jilin University, Changchun, China, in 2016. He is currently pursuing the Ph.D. degree. His research interests include traffic flow simulation and cooperative eco-driving strategy for vehicles.





Guoyuan Wu (Senior Member, IEEE) received the Ph.D. degree in mechanical engineering from the University of California at Berkeley, Berkeley. He is currently an Associate Researcher and an Associate Adjunct Professor with the Bourns College of Engineering—Center for Environmental Research and Technology and the Department of Electrical and Computer Engineering, University of California at Riverside, respectively. His research interests include connected and automated transportation systems, shared mobility, transportation electrification, the optimization and control of vehicles, traffic simulation, and emissions measurement and modeling.



Xiangmo Zhao (Member, IEEE) received the Ph.D. degree from Chang'an University, Xi'an, China, in 2006. He is currently the President of Xi'an Technology University and a Professor with the School of Information Engineering, Chang'an University. He is also the Vice President of the Joint Laboratory for Connected Vehicles, Ministry of Education and China Mobile, and the Shaanxi Road Traffic Intelligent Detection and Equipment Engineering Technology Research Centre. His research interests include connected vehicles, automated vehicles, and intelligent transportation systems. He is the Director of the Information Professional Committee, a member of the Advisory Expert Group of the China Transportation Association, a member of the National Motor Vehicle Operation Safety Testing Equipment Standardization Committee and the Leading Group of the National Traffic Computer Application Network, the Vice Chairperson of the Institute of Highway Association on Computer Professional Committee, and the Deputy Director of the Institute of Computer in Shaanxi Province.



Muhammet Deveci received the B.Sc. degree in industrial engineering from Cukurova University, Adana, Turkey, in 2010, and the Ph.D. degree in industrial engineering from Yildiz Technical University, Istanbul, Turkey, in 2017. He is currently an Honorary Senior Research Fellow with the Bartlett School of Sustainable Construction, University College London, U.K., and he is also a Visiting Professor with the Royal School of Mines, Imperial College London, London. He is also an Associate Professor with the Department of Industrial Engineering, Turkish Naval Academy, National Defence University, Istanbul. He has published over 120 papers in journals indexed by SCI/SCI-E papers at reputable venues. He is also an Editorial Board Member of *INS*, *ASOC*, *EAAI*, *ESWA*, and *AIR*. Based on the 2020 and 2021 publications from Scopus and Stanford University, he is within the world's top 2% scientists in the field of artificial intelligence.